DISINTEGRATION OF A LIQUID JET

V. A. Ivanov

Zhurnal Prikladnoi Mekhaniki i Tekhnicheskoi Fiziki, Vol. 7, No. 4, pp. 30–37, 1966

A number of theoretical and experimental studies [1–7] have been devoted to the problem of the disintegration of a liquid jet flowing into a gas medium. However, the disintegration process has been studied only at low exit velocities. Moreover, all the theoretical analyses have been based on the method of small perturbations, with the assumption that the surface deformations are small as compared with the initial radius of the jet. The author has attempted an experimental and theoretical study of jet disintegration without assuming that the deformations are small.

Figure 1 shows the basic disintegration characteristic–the length of the continuous part of the jet L (mm)–as a function of the exit velocity U_0 (m/sec) [1].

The linear initial section corresponds to disintegration under the influence of capillary forces: the time required for the jet to break down into droplets is constant. The effect of a gas medium is to reduce the disintegration time. The curve has a first extremum and a descending branch.

In this range of velocities the surface deformations of the jet are mainly axisymmetric. Asymmetric perturbations, which beyond a certain transition velocity give rise to wavelike deformations, are also observed. An experimental dependence for this range of velocities was first obtained in [1].

The first analysis for an ideal liquid was made by Rayleigh [2], and for a viscous liquid by Weber [1]. However, the investigation of disintegration over a wider range of velocities is of particular practical interest. New experimental results have recently been obtained [3, 4].

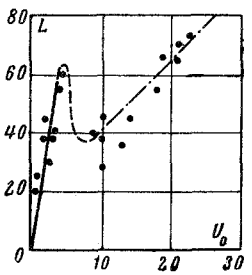

Fig. 1

Figure 2 shows the length L (mm) of the continuous part of the jet [4] at velocities corresponding to a pressure drop p from zero to one thousand atmospheres. The curve has two linear sections and five extrema.

The existing studies do not explain these experimental results. The reason is that the electro-contact method [4] of determining the continuous part at high-velocities does not permit the representation of the disintegration process as a whole, and at high velocities ordinary photography is not very effective. Lack of understanding of the disintegration process has so far prevented the development of a theoretical model of the disintegration effect in the region of wavelike deformations.

Accordingly, the author has designed and carried out the following experiments. A jet of water flowed from a nozzle at a velocity calculated to give a sharp image in frame photography. A relative velocity of the jet and medium was obtained by creating an accompanying flow or counterflow. This made it possible to obtain sharp photographs of the deformation processes corresponding to high exit velocities, namely, axisymmetric disintegration (Fig. 3), wavelike deformations (Fig. 4), and the beginning of atomization (Fig. 5). In addition, the length of the continuous part of the jet was measured by the electro-contact method in the absence of an artificial gas flow. To establish the three-dimensional shape of the jet, it was filmed in two projections.

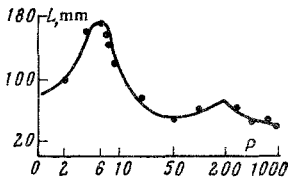

Fig. 2

The following results, which supplement the known disintegration picture [1], were obtained. In the case of wavelike deformations, after the appearance of kinks (by a "kink" we mean an element of the twisted jet) axisymmetric deformations, which determine the disintegration time, begin to develop in the jet. At first, kinks developed in planes passing through the axis of the jet. Subsequently, interaction of these kinks distorts their original plane shape.

In the presence of large initial perturbations (forced oscillations of the nozzle) the wavelength is determined by these perturbations. The experiments made it possible to clarify the nature of the curve shown in Fig. 2.

The first minimum corresponds to the appearance of wavelike deformations. The wavy jet produces an accompanying motion of the surrounding medium. In this case the relative velocity falls, and the ensuing axisymmetric deformations lead to disintegration of the jet. The second linear section corresponds to capillary disintegration and is similar to the first section. This linear section is followed by a second maximum and a descending branch due to the influence of the gas-dynamic force.

With increase in velocity the surface of the jet becomes unstable for short waves, leading to the separation of droplets. This causes even greater entrainment of the surrounding medium. The length of the jet again increases, reaches a third maximum, and decreases.

In the presence of axisymmetric deformations cosinusoidal surface shapes and shapes with a cylindrical central section are observed. The deformation of the latter is interrupted by the appearance of perturbations on the cylindrical part before disintegration.

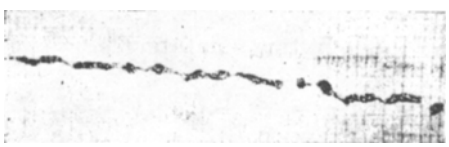

Fig. 3

In the presence of wavelike deformations the curvature of the jet forces the enveloping gas flow to accelerate on the convex sections, which leads to the development of kinks. The frontal part of a developed kink is deformed by a counterflow, leading to the formation of jet shapes resembling steps and loops.

§1. We shall first consider axisymmetric deformations. A jet of incompressible fluid of radius a and density ρ_1 moves relative to another incompressible fluid of density ρ_2 at the constant velocity U_0, σ is the

surface tension at the interface. By virtue of the symmetry of the problem the equations of motion may conveniently be written in a cylindrical coordinate system

$$\frac{du}{dt} = -\frac{1}{\rho_1}\frac{\partial p}{\partial z} + \nu\left[\frac{\partial^2 u}{\partial z^2} + \frac{1}{r}\frac{\partial}{\partial r}\left(r\frac{\partial u}{\partial r}\right)\right], \quad (1.1)$$

$$\frac{dv}{dt} = -\frac{1}{\rho_1}\frac{\partial p}{\partial r} + \nu\left[\frac{\partial^2 v}{\partial z^2} + \frac{\partial}{\partial r}\left(\frac{1}{r}\frac{\partial rv}{\partial r}\right)\right]; \quad (1.2)$$

the equation of continuity is

$$\frac{\partial u}{\partial z} + \frac{1}{r}\frac{\partial}{\partial r}(rv) = 0. \quad (1.3)$$

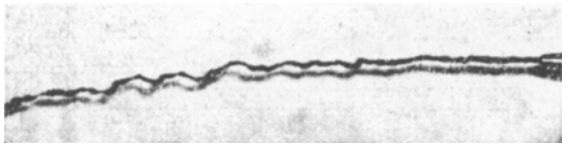

Fig. 4

Here v is the radial velocity component, and u is the component in the direction of the jet axis. We introduce the dimensionless quantities

$$z_1 = \frac{z}{l_0}, \quad u_1 = \frac{u}{u^\circ}, \quad v_1 = \frac{v}{v^\circ}, \quad r_1 = \frac{r}{a}, \quad t_1 = \frac{t}{T}. \quad (1.4)$$

Here l_0 is the wavelength of the perturbation, u° is the average velocity over the cross section, v° is the average rate of deformation, and T is the disintegration time.

From (1.3) it follows that

$$v^\circ = \frac{u^\circ a}{l_0}. \quad (1.5)$$

Substituting (1.4) and (1.5) in (1.1) and (1.2), at T = $= l_0/u^\circ$ we obtain

$$\left[\frac{u^{\circ 2}}{l_0}\right]\frac{\partial u_1}{\partial t_1} + \left[\frac{u^{\circ 2}}{l_0}\right]u_1\frac{\partial u_1}{\partial z_1} + \left[\frac{u^{\circ 2}}{l_0}\right]v_1\frac{\partial u_1}{\partial r_1} = -\frac{1}{\rho_1}\frac{\partial p}{\partial z} + \nu\left\{\left[\frac{u^\circ}{l_0^2}\right]\frac{\partial^2 u_1}{\partial z_1^2} + \left[\frac{u^\circ}{a^2}\right]\frac{1}{r_1}\frac{\partial}{\partial r_1}\left(r_1\frac{\partial u_1}{\partial r_1}\right)\right\},$$

$$\left[\frac{u^{\circ 2}a}{l_0^2}\right]\frac{\partial v_1}{\partial t} + \left[\frac{u^{\circ 2}a}{l_0^2}\right]u_1\frac{\partial v_1}{\partial z_1} + \left[\frac{u^{\circ 2}a}{l_0^2}\right]v_1\frac{\partial v_1}{\partial r_1} = -\frac{1}{\rho_1}\frac{\partial p}{\partial r} + \nu\left\{\left[\frac{u^\circ a}{l_0^3}\right]\frac{\partial^2 v_1}{\partial z_1^2} + \left[\frac{u^\circ}{l_0 a}\right]\frac{1}{r_1}\frac{\partial}{\partial r_1}(r_1 v_1)\right\}.$$

When $l_0 \gg a$, omitting small terms, we have

$$\frac{\partial u}{\partial t} + u\frac{\partial u}{\partial z} + v\frac{\partial u}{\partial r} = -\frac{1}{\rho_1}\frac{\partial p}{\partial z} + \nu\frac{1}{r}\frac{\partial}{\partial r}\left(r\frac{\partial u}{\partial r}\right),$$

$$\frac{\partial p}{\partial r} = 0. \quad (1.6)$$

We shall neglect the variation of axial velocity over the cross section of the jet, and work with the average velocity u°. Omitting the unimportant superscript, from (1.6) we obtain

$$\frac{\partial u}{\partial t} + u\frac{\partial u}{\partial z} = -\frac{1}{\rho_1}\frac{\partial p}{\partial z}. \quad (1.7)$$

Thus, we have eliminated the viscosity terms from the equation of motion. Nevertheless, in the final solution the viscosity effect is taken into account in the relation for the wavelength of the perturbation. We represent the radius of the free surface R in the form (Fig. 6)

$$R = a_0 + a_1\cos kz. \quad (1.8)$$

From the constant-volume condition it follows that

$$a^2 = a_0^2 + {}^1/_2 a_1, \quad a\sqrt{{}^2/_3} \leqslant a_0 \leqslant a,$$

$$0 \leqslant a_1 \leqslant \sqrt{{}^2/_3}\,a. \quad (1.9)$$

Instead of (1.3) in our approximation it is more convenient to write

$$\frac{\partial S}{\partial t} + \frac{\partial}{\partial z}(Su) = 0 \qquad (S = \pi R^2). \quad (1.10)$$

Integrating (1.10) with respect to z with the following boundary conditions:

$$z = 0, \ u = 0 \qquad z = {}^1/_2 l_0, \qquad u = 0$$

and using (1.9), we obtain, neglecting $\partial a_0/\partial t$,

$$u = -\frac{1}{kR^2}\frac{\partial a_1}{\partial t}\left(2a_0\sin kz + \frac{1}{2}a_1\sin 2kz\right). \quad (1.11)$$

Substituting (1.11) into (1.7) and integrating with respect to z, for the dimensionless displacement h = $= a_1/a$ we obtain the equation

$$\frac{\partial^2 h}{\partial t^2} + \left[\frac{1}{h} - \frac{4h}{(1-h^2)^2}\left(\frac{1}{h}\ln\frac{1-h}{1+h} - \frac{2}{1-h^2}\right)^{-1}\right]\left(\frac{\partial h}{\partial t}\right)^2 = \frac{(p_0 - p)k^2}{\rho_1}\left(\frac{1}{h}\ln\frac{1-h}{1+h} - \frac{2}{1-h^2}\right)^{-1} \quad (1.12)$$

which is linear in $(\partial h/\partial t)^2$. Here the value p_0 corresponds to z = 0, and p to the value $z = l_0/2$.

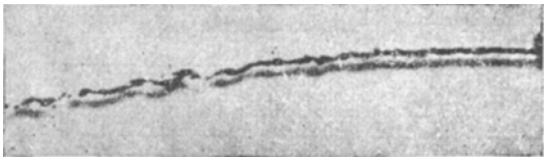

Fig. 5

The pressure p is expressed in terms of the principal radii of curvature of the normal section, R_1 and R_2, as follows:

$$p = \sigma\lambda = \sigma\,(1/R_1 + 1/R_2).$$

We can simplify the expression

$$\lambda = \frac{(1+m^2)\,t + (1+q^2)\,r - 2rqs}{(1+q^2+m^2)^{3/2}}$$

$$\left(m = \frac{\partial f}{\partial x}, \quad s = \frac{\partial^2 f}{\partial x \partial z}, \quad q = \frac{\partial f}{\partial z}, \quad r = \frac{\partial^2 f}{\partial x^2}, \quad t = \frac{\partial^2 f}{\partial z^2}\right)$$

for the surface $y = f(z, x) = [R^2(z) - x^2]^{1/2}$ in the case of axisymmetric deformations. Without loss of generality, we set x = 0; then

$$\lambda = \frac{\partial^2 R}{\partial z^2}\left[1 + \left(\frac{\partial R}{\partial z}\right)^2\right]^{-3/2} + \frac{1}{R}\left[1 + \left(\frac{\partial R}{\partial z}\right)^2\right]^{-1/2}.$$

Using (1.8), in the region of capillary disintegration we obtain

$$p_0 - p = 2\sigma ak^2\left[1 - \frac{1}{a^2k^2(1-h)}\right]h. \qquad (1.13)$$

Passing to the new independent variable $\tau = k^2t\sqrt{2a\sigma/\rho_1}$ from Eq. (1.12) (with the initial conditions $h = h_0$ and $dh/d\tau = 0$ at $\tau = 0$), we obtain

$$\tau = \tau(ka, h_0). \qquad (1.14)$$

The effect of the initial perturbations on the disintegration time is estimated using the simplified equation with $h \ll 1$:

$$\frac{\partial^2 h}{\partial \tau^2} + \frac{1}{h}\frac{\partial h}{\partial \tau} = \frac{(1-a^2k^2)}{4a^2k^2}h. \qquad (1.15)$$

For the initial deformation period the solution of (1.15) has the form

$$\tau = ak\left(\frac{2}{1-a^2k^2}\right)^{1/2}\ln\left(\frac{2h^2}{h_0^2}\right). \qquad (1.16)$$

§2. We shall consider the effect of the surrounding medium on the disintegration time. We assume that the surrounding gas is inviscid and incompressible. In view of the symmetry of motion the velocity potential satisfies the equation

$$\Delta\varphi = \frac{\partial^2\varphi}{\partial z^2} + \frac{1}{r}\frac{\partial}{\partial r}\left(r\frac{\partial\varphi}{\partial r}\right) = 0. \qquad (2.1)$$

For convenience, we shall assume that the jet is stationary, while the gas moves at velocity U_0 at infinity. The expression

$$\varphi = \beta K_0(kr)\sin kz - U_0 z \qquad (2.2)$$

will be the solution of (2.1) satisfying this condition; K_0 is a zero-order Macdonald function.

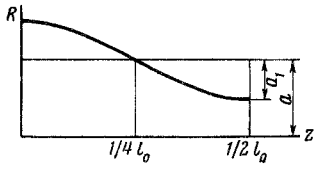

Fig. 6

For the velocities we obtain

$$v = -\frac{\partial\varphi}{\partial r} = -\beta k K_0'(kr)\sin kz,$$
$$u = -\frac{\partial\varphi}{\partial z} = -\beta k K_0(kr)\cos kz + U_0.$$

Considering that the velocity of longitudinal motion is much greater than the transverse velocity, while the variation of R along the length is large if the deformations are considerable, we can write the boundary condition at the free surface in the form

$$v = \frac{\partial R}{\partial t} + \frac{\partial R}{\partial z}U_0 \approx \frac{\partial R}{\partial z}U_0 \qquad \text{at } r = R. \qquad (2.3)$$

From (1.8) and (2.3), substituting for R its mean value over the length a, we obtain

$$\beta = a_1\frac{U_0}{K_0'(ka)}. \qquad (2.4)$$

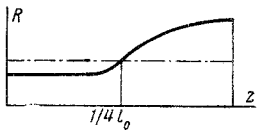

Fig. 7

The pressure is found from

$$p = \rho_2\frac{\partial\varphi}{\partial t} - \frac{1}{2}\rho_2(v^2+u^2),$$
$$p = \rho_2\frac{\partial\beta}{\partial t}K_0(ka)\sin kz - \frac{1}{2}\rho_2[k^2\beta^2K_0'^2(ka)\sin^2 kz + U_0^2 -$$
$$- 2U_0\beta K_0'(ka)k\cos kz + \rho_2\beta^2k^2K_0^2(ka)\cos^2 kz]. \qquad (2.5)$$

The pressure drop between the points $z = 0$ and $z = l_0/2$ is equal to

$$p - p_0 = \rho_2U_0^2ka\frac{K_0(ka)}{K_0'(ka)}h\left[2 - ak\frac{K_0(ka)}{K_0'(ka)}h\right]. \qquad (2.6)$$

When $h \ll 1$

$$p - p_0 = 2\rho_2U_0^2\frac{K_0(ka)}{K_0'(ka)}kah. \qquad (2.7)$$

From (1.13) and (2.7) at $h \ll 1$ we obtain the condition for the appearance of axisymmetric deformations:

$$\varkappa^2 = \rho_2\frac{U_0^2a}{\sigma} = ka\left(\frac{a^2k^2-1}{a^2k^2}\right)\frac{K_0'(ka)}{K_0(ka)}. \qquad (2.8)$$

When $U_0 = 0$ we get disintegration under the influence of capillary forces. This corresponds to $ak = 1$.

All perturbations longer than specified by condition (2.8) are unstable. However, the highest deformation rate is possessed by waves of a perfectly definite length. The corresponding condition is obtained from (1.12), (1.13), and (2.7):

$$\frac{\partial}{\partial(ka)}(p_0 - p) = 0. \qquad (2.9)$$

The general expression for the optimal wave number k is complicated, but, considering that in the range in question (up to the appearance of wavelike deformations) $K_0(ka)/K_0'(ka)$ varies only slightly, for a jet of low-viscosity fluid we can obtain approximately

$$ka = \frac{3}{4}\frac{K_0(ka)}{K_0'(ka)}\varkappa^2 + \left(\frac{9}{16}\frac{K_0^2(ka)}{K_0'^2(ka)}\varkappa^4 + \frac{1}{2}\right)^{1/2}. \qquad (2.10)$$

For the optimal deformations under the influence of capillary forces the value $\varkappa = 0$ gives the results obtained by Rayleigh [2]:

$$ka = \frac{1}{\sqrt{2}}, \qquad l_0 = \frac{2\pi}{k} = 2\sqrt{2}\pi a. \qquad (2.11)$$

For a viscous fluid the wavelength of the optimal deformation was obtained by Weber [1]:

$$\frac{l_0}{2a} = \pi\left[2\left(1+\frac{3\eta_1}{\sqrt{2\sigma\rho_1 a}}\right)\right]^{1/2} = \pi\left[2\left(1+\frac{3W}{R}\right)\right]^{1/2}$$

$$W = U_0\left(\frac{2\rho_1 a}{\sigma}\right)^{1/2}, \qquad R = \frac{2U_0\rho_1 a}{\eta_1}. \qquad (2.12)$$

Here η_1 is the viscosity of the fluid, W is the Weber number, and R is the Reynolds number.

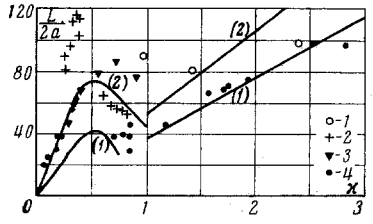

Fig. 8

The equation of equilibrium of the gas-dynamic and capillary forces for the curved jet [5]

$$\frac{\sigma}{a}[1 - s^2 - (ka)^2] = \rho_2 akU_0^2\frac{K_s(ka)}{K_s'(ka)}$$

enables us to obtain the velocity of transition to wavelike deformations. In this case

$$s = 1, \qquad ka \ll 1, \qquad \frac{K_1(ka)}{K_1'(ka)} \approx -ka,$$

$$\varkappa = U_0\left(\frac{\rho_2 a}{\sigma}\right)^{1/2} = 1. \qquad (2.13)$$

In the general case of symmetrical disintegration $p_0 - p$ in expression (1.4) represents the sum of (1.13) and (2.6).

§3. We shall now consider wavelike deformations. With the appearance in the jet of wavelike perturbations the relative velocity of the jet and the medium begins to decrease. This leads to the appearance of axisymmetric deformations with a different wavelength. When the relative velocity is reduced by an accompanying flow, the deformations with $ka > 1$ must be suppressed by the surface tension. However, observation shows that such deformations are not suppressed. The cosinusoidal shape of the surface becomes unstable, and is replaced with an axisymmetric shape with a central cylindrical section (see Fig. 7). For such shapes the variation of the radius of the free surface at $0 \leq z \leq l_0/4$ is only slight. Thus, after integrating with respect to z with boundary conditions $u = 0$ at $z = 0$, we can obtain from (1.11) the following expression for the velocity:

$$u = -2\frac{z}{R}\frac{\partial R}{\partial t}. \qquad (3.1)$$

We substitute (3.1) in (1.7) and integrate (1.7) with respect to z in the interval from 0 to $l_0/4$:

$$\frac{l_0^2}{16R}\left[\frac{3}{R}\left(\frac{\partial R}{\partial t}\right)^2 - \frac{\partial^2 R}{\partial t^2}\right] = \frac{p_0 - p}{\rho_1}. \qquad (3.2)$$

For the pressure drop we have

$$z = 0, \quad p_0 = \frac{\sigma}{R},$$

$$z = \frac{l_0}{4}, \quad p = \frac{\sigma}{a}, \quad p_0 - p = \frac{\sigma(a-R)}{aR}. \qquad (3.3)$$

We transform Eq. (3.2) to dimensionless parameters:

$$\frac{\partial^2 h}{\partial\tau^2} - \frac{3}{h}\left(\frac{\partial h}{\partial\tau}\right)^2 = h - 1$$

$$\left(\tau = \frac{4}{l_0}\left(\frac{2\sigma}{\rho_1 a}\right)^{1/2} t, \; h = \frac{R}{a}\right). \qquad (3.4)$$

The solution of (3.4) with initial conditions $\partial h/\partial\tau = 0$, $h = h_0$ at $\tau = 0$ can be written in the form

$$\tau = \int_{h_0}^{0}\left[5h^2\left(\frac{h^4}{h_0^4} - 1\right) - 4h\left(\frac{h^5}{h_0^5} - 1\right)\right]^{-1/2} dh. \qquad (3.5)$$

Expression (3.5) determines the disintegration time of wavelike deformations on the linear section.

To estimate the effect of the initial perturbations we set $h = 1 + \Delta h$, with $\Delta h \ll 1$, and, neglecting the cubes of small quantities, from (3.4) we obtain

$$\tau = \frac{\ln h/h_0}{\sqrt{10}}. \qquad (3.6)$$

We shall now consider some examples.

1. The length of the continuous part of the jet in the region of capillary disintegration, in accordance with (1.14), is expressed as follows:

$$L = U_0 t = \frac{W}{2k^2 a}\tau(ka, h_0). \qquad (3.7)$$

In Heinlein's experiments [1] water with the characteristics: $\sigma/\rho_1 = 70.8$ cm^3/sec^2; $2a = 0.012$–0.104 cm was taken as the low-viscosity fluid.

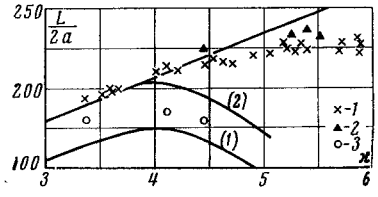

Fig. 9

The observed wavelengths of the axisymmetric perturbations had values $l_0/2a = 4.3$–7. The values of τ, computed for $h_0 = 10^{-2}$ and $h_0 = 10^{-3}$, corresponding in order of magnitude to the experiments of [6] and the measurements of [1], are

$$\tau_1 = 7.25, \quad L_1 = 11.7\ aW,$$

$$\tau_2 = 9.46, \quad L_2 = 23.6\ aW.$$

The calculated and experimental [1, 3, 4] results are presented in Fig. 8: 1) $2a = 1$ mm [4], 2) $2a = 0.66$ mm [7], 3) $2a = 0.54$ mm [3], 4) $2a = 0.51$ mm [1]; water.

The low-viscosity condition

$$3W/R \ll 1 \qquad (3.8)$$

for water is almost always satisfied.

2. When $3W/R \gg 1$ in the case of a high-viscosity fluid it follows from (1.12) that

$$Q \approx -\frac{2h}{a^2k^2(1-h^2)^2}\left(\frac{1}{h}\ln\frac{1-h}{1+h}-\frac{2}{1-h^2}\right)^{-1},$$

$$\tau = k\left(\frac{2\sigma}{a\rho_1}\right)^{1/2} t. \qquad (3.9)$$

Then

$$t = \frac{1}{k}\left(\frac{\rho_1 a}{2\sigma}\right)^{1/2}\tau(h_0). \qquad (3.10)$$

It follows from (3.10) that for the same initial jet radius the ratio t_1/t_2 for two high-viscosity fluids is given by

$$\frac{t_1}{t_2} = \frac{l_{01}W_1}{l_{02}W_2}. \qquad (3.11)$$

We shall compare the experimental results [1] for jets of glycerine and castor oil ($\sigma_1/\rho_1 = 35.7$ cm^3/sec^2; $\sigma_2/\rho_2 = 52.7$ cm^3/sec^2; $l_{01} = 60a$; $l_{02} = 12a$).

The ratio (3.11) gives a value $t_1/t_2 = 6$ corresponding to results of the experiments. Since

$$l_0 = 2a\pi\left(\frac{6W}{R}\right)^{1/2},$$

the time to disintegration

$$t = a\sqrt{6\eta_1}\left(\frac{2\sigma^3}{\rho_1 a}\right)^{-1/4} \sim a^{1.25}, \qquad (3.12)$$

which corresponds to experiment [1].

3. In the presence of wavelike deformations, toward the end of deformation the velocity of the axisymmetric deformations, in accordance with (3.4), slows. Observations show that in the final moments shortwave perturbations that break up the jet appear on the cylindrical section. Retardation of deformation begins to exert an effect at $h = 0.1$. Therefore the calculations were performed for $0.1 \leq h \leq h_0$.

We calculated values of τ at $h_0 = 0.99$ and $h_0 = 0.999$.

The corresponding values are $\tau_1 = 1.88$, $\tau_2 = 2.54$. The second maximum of the curve may be displaced along the linear section. Its position depends on the accompanying flow, determined by the number of kinks in the jet, which, in its turn, depends on the initial perturbations.

However, in each individual case the first and second maxima occur at the same value of $\varkappa$. This condition makes it possible to express the velocity corresponding to the maximum length of the continuous part in terms of the exit parameters:

$$U_0 \sim \left(\frac{\sigma}{2a\rho_2}\right)^{1/2}. \qquad (3.13)$$

Relation (3.13) is confirmed by experiments with diesel fuel [3].

On the section where gas-dynamic influences predominate (descending branch of curve) at $\varkappa \gg 1$ we have the following values of the time and range from (1.14) and (3.6), respectively:

$$t = \frac{l_0}{4\pi U_0}\left(\frac{\rho_1}{\rho_2}\right)^{1/2}\tau(h_0,\ ka), \qquad L = \frac{l_0}{4\pi}\left(\frac{\rho_1}{\rho_2}\right)^{1/2}\tau(h_0,\ ka).$$

The exit velocity exerts an effect only through the wavelength l_0.

There is a discrepancy between the condition for the occurrence of wavelike deformations (2.13) and experiment. This discrepancy may be related to the assumption that the medium can be replaced by an ideal fluid, whereas in reality the gas flow is turbulent.

For a low-viscosity fluid, instead of (2.13), the relation

$$\varkappa_1 = U_0\left(\frac{2\rho_2 a}{\sigma}\right)^{1/2} = 1$$

gives good agreement with experiment.

Figures 8 and 9 present the results of calculations for all sections of axisymmetric and wavelike deformations and the experimental results obtained by the author and in [1, 4, 7]. At large $\varkappa$ (Fig. 9) the values of $2a$ correspond to: 1) $2a = 2$ mm, 2) $2a = 4$ mm—author's experiments, 3) $2a = 1$ mm [4]; water.

REFERENCES

1. Collection: Internal Combustion Engines [in Russian], vol. 1, ONTI NKTP SSSR, 1936.

2. J. W. Rayleigh, Theory of Sound [Russian translation], vol. 2, OGIZ, 1944.

3. A. S. Lyshevskii, Laws of Atomization of Liquids in Mechanical Pressure Nozzles [in Russian], Novocherkassk, 1961.

4. L. F. Vereshchagin, A. A. Semerchan, and S. S. Sekoyan, "Decay of a high-speed water jet," ZhTF, 29, no. 1, 1959.

5. V. G. Levich, Physico-Chemical Hydrodynamics [in Russian], Fizmatgiz, 1959.

6. V. I. Blinov and E. L. Feinberg, "Pulsation of a jet and its disintegration into droplets," ZhTF, 3, no. 5, 1933.

7. Ya. K. Trotskii, "Disintegration of a liquid jet into droplets," ZhTF, 3, no. 5, 1933.

15 June 1965 Moscow